Supporting Information

Redding et al. 10.1073/pnas.1419672112

SI Text

Modeling Mode Competition and Lasing Thresholds in Chaotic Cavities

The ability to achieve highly multimode lasing at a moderate pump value depends on two factors: a relatively uniform Q distribution and minimized mode competition. We used the steady-state ab initio laser theory (SALT) to understand the role of both of these factors in D-shaped cavities and optimize the geometry to enable highly multimode lasing. SALT first calculates the noninteracting modal thresholds and then updates these thresholds in the presence of modal interactions as the pumping of the gain medium is increased. The noninteracting lasing thresholds incorporate both effects of the mode decay rate and the distance of its frequency from the center of the gain spectrum and can be calculated as

$$D_n = \eta_n \left(\frac{k_n - k_a + i\gamma_\perp}{\gamma_\perp} \right), \qquad \textbf{[S1]}$$

where D_n is the noninteracting threshold of the nth mode, k_n is lasing mode frequency, k_a is the center frequency of the gain spectrum, $\gamma_\perp$ is the width of the gain spectrum, and η_n is the threshold constant flux (TCF) eigenvalue of the associated cavity resonance (1). The TCF eigenvalue can be calculated for a homogeneous dielectric cavity with uniform pumping, such as the ones studied here, as

$$\eta_n = \varepsilon_c \left(\frac{(k_n - i\gamma_n/2)^2}{k_n^2} - 1 \right), \qquad \textbf{[S2]}$$

where ε_c is the passive cavity dielectric constant and γ_n is the intensity decay rate of the nth mode, which can be calculated from the Q factor,

$$Q_n = \frac{k_n}{\gamma_n}. \qquad \textbf{[S3]}$$

Qualitatively speaking, for the high-Q cavities studied here, η_n contains information about the decay rate of the nth lasing mode, which must be compensated for to achieve lasing, whereas the term in the parentheses in Eq. **S1** adjusts this value due to the distance between the lasing mode frequency and the center of the gain spectrum. Although the TCF eigenvalue and the distance from the center of the gain spectrum are both complex quantities, the noninteracting threshold is reached when the imaginary components of these factors cancel exactly, allowing for a positive, real threshold, D_n. Above threshold, the lasing modes satisfy a set of coupled, nonlinear, differential equations. SALT facilitates the solution of these equations by assuming that the lasing modes are operating in the continuous wave regime.

Fig. S1*A* shows the Q distribution for each of the cavity modes, clearly showing that the D-shaped cavities exhibit a far more uniform Q distribution than the circular microcavity. In Fig. S1*B*, we show the lasing thresholds for each cavity type without normalization. Note that Fig. 1*E* in the main text is a normalized version of these same data. As expected, the circular microdisk shows the lowest lasing threshold, because it supports the highest Q mode. However, in the circular cavity the threshold increases dramatically for higher-order modes and the pump value required to turn on all of the first 10 modes is actually higher in the circular cavity than in the D-shaped cavity with $r_0 = 0.5R$.

Experimental Characterization and Comparison of Fabry–Perot Cavity, Circular Cavity, and D-Shaped Cavity Lasers

Four cavity shapes were fabricated on the same wafer: a 100-μm × 2-mm Fabry–Perot cavity, a 100-μm radius circular microdisk, a 100-μm radius D-shaped cavity with $r_0 = 0.5R$, and a 500-μm radius D-shaped cavity with $r_0 = 0.5R$. The emission spectra below and above the lasing threshold are presented in Fig. S2 for each cavity. In addition, the speckle pattern formed by lasing emission coupled into a multimode fiber is also shown for each cavity in Fig. S2. Although the FP cavity supported ∼450 transverse modes, strong mode competition limited lasing to ∼3 mutually incoherent transverse modes. Similarly, the number of lasing modes in the circular microdisk was limited to ∼15 due to strong mode competition, whereas the D-shaped cavity with the same radius supported ∼100 mutually incoherent modes. This illustrates the advantage of using a chaotic cavity shape to enable highly multimode lasing in a cavity with a fixed size. Finally, the 500-μm radius D-shaped cavity supported ∼1,000 lasing modes, producing very low-contrast speckle, appropriate for full-field imaging.

1. Ge L, Chong YD, Stone AD (2010) Steady-state ab initio laser theory: Generalizations and analytic results. *Phys Rev A* 82(6):063824.

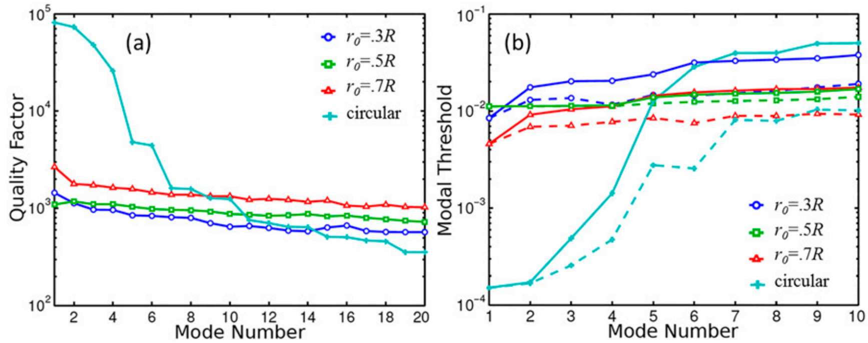

Fig. S1. (*A*) Calculated quality factors for the 20 highest-*Q* modes in three D-shaped cavities and a circular cavity of the same radius. The cavity parameters are identical to those in Fig. 1. The D-shaped cavity with $r_0 = 0.5R$ has the most uniform *Q* distribution. (*B*) Calculated lasing thresholds without mode competition (dashed lines) and with mode competition (solid lines) for three D-shaped cavities and a circular cavity. Although the circular cavity has the lowest threshold for the first few lasing modes, it has the highest thresholds for the 7–10th lasing modes due to uneven *Q* distribution and strong mode competition for gain. In contrast, the D-shaped cavities, and in particular the optimal one with $r_0 = 0.5R$, exhibit much more uniform thresholds for the first 10 lasing modes. Thus various D cavities are distinguished primarily by the different strengths of mode competition in each.

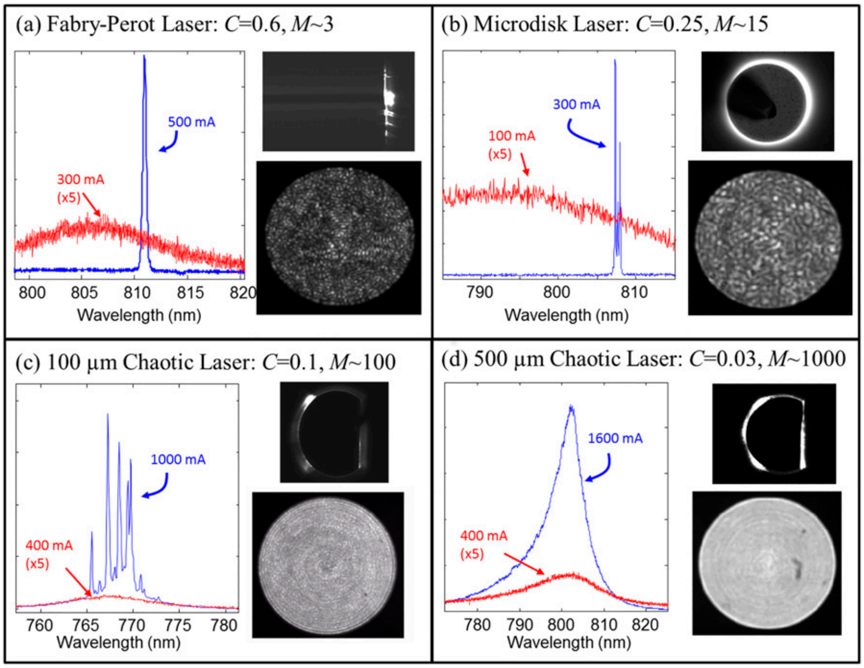

Fig. S2. Characterization of four lasers with different cavity shapes fabricated on the same wafer. The emission spectra below and above lasing threshold are shown for each cavity along with a top-view microscope image of the cavity and an image of the speckle pattern formed at the end of a multimode fiber. The speckle contrast, *C*, and the number of mutually incoherent lasing modes, *M*, are listed for each laser. Strong mode competition in the Fabry–Perot cavity (*A*) and the circular microdisk (*B*) limit lasing to ∼3 and ∼15 modes, respectively. On the other hand, the chaotic cavity lasers support highly multimode lasing, with the 100-μm radius D-shaped cavity (*C*) supporting ∼100 modes and the 500-μm radius D-shaped cavity (*D*) supporting ∼1,000 modes.